

# $\pi$ junction qubit in monolayer graphene

Colin Benjamin and Jiannis K. Pachos

*Quantum Information Group, School of Physics and Astronomy,  
University of Leeds, Woodhouse Lane, Leeds LS2 9JT, UK.*

We propose to combine the advantages of graphene, such as easy tunability and long coherence times, with Josephson physics to manufacture qubits. If these qubits are built around a 0 and  $\pi$  junction they can be controlled by an external flux. Alternatively, a d-wave Josephson junction can itself be tuned via a gate voltage to create superpositions between macroscopically degenerate states. We show that ferromagnets are not required for realizing  $\pi$  junction in graphene, thus considerably simplifying its physical implementation. We demonstrate how one qubit gates, such as arbitrary phase rotations and the exchange gate, can be implemented.

## I. INTRODUCTION

Graphene, a monatomic layer of graphite exhibits promising electronic properties that can be employed for quantum technologies<sup>1</sup>. Characteristically, its low energy excitations are described by the Dirac equation, it has a zero band gap, electronic speeds can reach a hundredth of the speed of light and it supports long range phase coherence. However it has not yet been utilised to create qubits suitable for quantum computation, apart from a proposal which meshes it with bilayer structures<sup>2</sup>. Here we show that a key ingredient of Josephson qubits, a  $\pi$ -junction<sup>3</sup> can be easily generated in graphene by application of a gate voltage alone. We establish a parametric regime for observing this effect and show how to manufacture qubits. These Josephson qubits can be used to perform single quantum gates, such as the phase and exchange gates. This opens up the possibility of employing graphene and utilizing its advantages for quantum information processing<sup>4</sup>.

The physical system we employ consists of a graphene substrate with superconducting correlations induced in

sections via the proximity effect<sup>5</sup> or by turning graphene superconducting<sup>11</sup> via doping. It comprises of two d-wave Josephson junctions (distinguished by their ground states, one at a phase difference  $\phi = 0$  and the other at  $\phi = \pi$ ), arranged as in Fig. 1(a). The total energy of the system is controlled by the flux,  $\Phi$ , that passes through the ring. The reversal of super-current in a Josephson device, where the free energy has global minima at phase difference  $\phi = \pi$ , is referred to as  $\pi$  shift. The corresponding Josephson junction is termed a  $\pi$  junction. This is in contrast to a 0 junction wherein the free energy has a global minimum at phase difference  $\phi = 0$ <sup>6</sup>. To be able to encode a qubit we have to construct a  $\pi$  junction and integrate it with the rest of our device (the 0 junction). A  $\pi$  junction is needed to create a doubly degenerate ground state, where a qubit is encoded. Here we demonstrate that a  $\pi$  junction can be identified in our system without the need of any ferromagnetic elements<sup>7</sup>, thus greatly simplifying its experimental implementation. In Fig. 1(b) we depict a simple d-wave graphene Josephson junction, which has two degenerate ground states, that can encode a qubit. In particular, we prove that a complete set of single qubit gates can be efficiently implemented demonstrating that our proposal is promising for quantum computation.

In Fig. 2, we show our graphene  $\pi$  junction set-up. It is known that with s-wave superconductors a  $\pi$  junction is not possible<sup>8</sup>. However, a Josephson junction with d-wave superconductors can exhibit a  $\pi$  shift<sup>9</sup>. Thus, we consider d-wave correlations in the superconducting segments (see Fig. 1).

## II. THEORY

The kinematics of quasi-particles in graphene is described by the Dirac-Bogoliubov-de Gennes equation<sup>10</sup>, which assumes the form

$$\begin{pmatrix} \hat{H} - E_F \hat{I} & \Delta \hat{I} \\ \Delta^\dagger \hat{I} & E_F \hat{I} - \hat{T} \hat{H} \hat{T}^{-1} \end{pmatrix} \Psi = E \Psi, \quad (1)$$

where  $E$  is the excitation energy,  $\Delta$  is the superconducting gap of a d-wave superconductor,  $\Psi$  is the wavefunc-

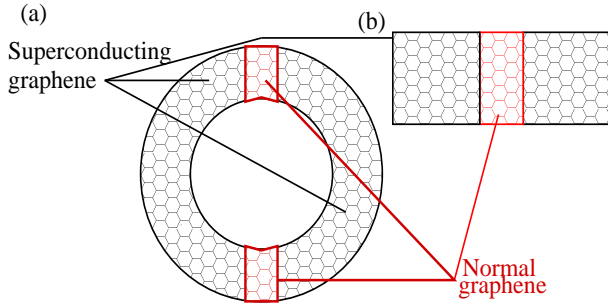


FIG. 1: (Color online) An overview of the set-up. (a) Two semicircular d-wave superconducting graphene strips (Gs) with normal graphene layers on top and bottom enclosing a magnetic flux,  $\Phi$ . By the application of suitable gate voltages to the normal graphene strip the junctions are tuned to either  $\phi = 0$  or  $\pi$  phase shift. (b) A graphene d-wave Josephson junction. For relatively small intervening length between the superconducting graphene one can have situations wherein degenerate ground states are formed and are pliable to external control via a gate voltage.

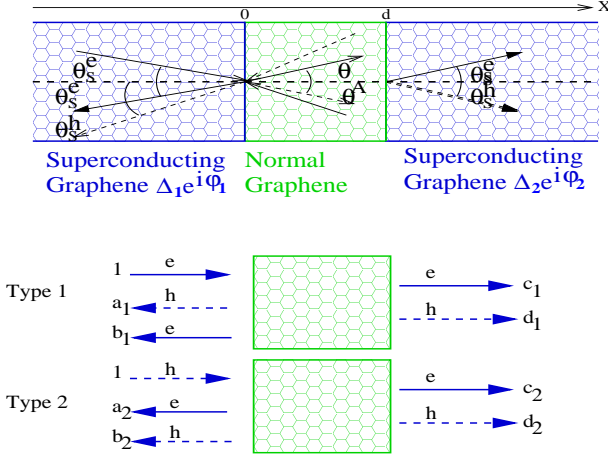


FIG. 2: (Color online) The Furusaki-Tsukada approach and the processes involved. Top:  $\theta_S^e$  is the angle of incidence of electron-like quasiparticle, while  $-\theta_S^e$  is the angle of its reflection. Hole-like quasiparticle are Andreev reflected at angle  $\theta^h$ . In the normal region electron and holes are transmitted and incident with angles  $\theta$  and  $\theta^A$ . Bottom: In type 1 process an electron-like quasiparticle is incident from the left, while in type 2 process a hole-like quasiparticle is incident from the left.  $a_1, b_2, d_1$  and  $d_2$  are amplitudes of hole-like quasiparticle, while  $a_2, b_1, c_1$  and  $c_2$  are scattering amplitudes for electron-like quasiparticles.

tion and  $\hat{\tau}$  represents  $4 \times 4$  matrices. In the above equation

$$\hat{H} = \begin{pmatrix} H_+ & 0 \\ 0 & H_- \end{pmatrix}, \quad H_{\pm} = -i\hbar v_F (\sigma_x \partial_x \pm \sigma_y \partial_y) + U. \quad (2)$$

Here  $\hbar, v_F$  (set equal to unity hence forth) are the Planck's constant and the energy independent Fermi velocity for graphene, while the  $\sigma$ 's denote Pauli matrices that operate on the sub-lattices  $A$  and  $B$ . The electrostatic potential  $U$  can be adjusted independently via a gate voltage or doping. We assume  $U = 0$ , in the normal region, while  $U = -U_0$  in the superconducting graphene. In our work we consider  $U_0 = 100\Delta$ . Further we choose d-wave superconducting correlations which imply a type II (or high  $T_c$ ) superconductor. This is most likely to be observed in graphene<sup>11</sup>. The subscripts of Hamiltonian  $\pm$  refer to the Fermi points  $K_+$  and  $K_-$  in the Brillouin zone.  $T = -\tau_y \otimes \sigma_y C$ , ( $C$  being complex conjugation) is the time reversal operator, with  $\tau$  being Pauli matrices that operate on the  $\pm$  space and  $\hat{I}$  is the identity matrix.

To calculate the Josephson supercurrent, Free energy and show the formation of a  $\pi$  junction we proceed by first calculating the scattering wave functions of our system. Let us consider (Type 1 scenario in Fig. 2) an incident electron-like quasiparticle<sup>12</sup> from the left superconductor with pairing gap  $\Delta(\theta^+)e^{i\phi_1^+}$  ( $x < 0$ ) and energy  $E$ . For a right moving electron-like quasiparticle with an incident angle  $\theta$  the eigenvector and corresponding momentum read  $\Psi_{S_1+}^e = [u_e, u_e e^{i\theta^+}, v_e e^{-i\phi_1^+}, v_e e^{i(\theta^+ - \phi_1^+)}]^T e^{iq^e \cos \theta^+ x}$ ,  $q^e = (E_F + U_0 + \sqrt{E^2 - |\Delta(\theta^+)|^2})$ . A left moving

electron-like quasiparticle is described by the substitution  $\theta \rightarrow \pi - \theta$ . If Andreev-reflection takes place, a left moving hole-like quasiparticle is generated with energy  $E$ , angle of reflection  $\theta^-$  and its corresponding wavefunction is given by  $\Psi_{S_1-}^h = [v_h, -v_h e^{-i\theta^-}, u_h e^{-i\phi_1^-}, -u_h e^{-i(\theta^- + \phi_1^-)}]^T e^{-iq^h \cos \theta^- x}$ ,  $q^h = (E_F + U_0 - \sqrt{E^2 - |\Delta(\theta^-)|^2})$ . The quasi-particle wavevectors can also be expressed as  $q^{e/h} = E_F + U_0 \pm 1/\xi$ , where  $\xi$  is the coherence length. For the Dirac-Bogoliubov de Gennes equations to hold the Fermi wavelength in the superconductor  $1/(E_F + U_0)$  should be much smaller than the coherence length. The superscript e (h) denotes an electron-like (hole-like) excitation. Since translational invariance in the  $y$ -direction holds the corresponding component of momentum is conserved. This condition allows for the determination of the Andreev reflection angle  $\theta^-$  through  $q^h \sin(\theta^-) = q^e \sin(\theta^+)$ . The coherence factors are given by  $u_{e/h} = \sqrt{(1 + \sqrt{1 - |\Delta(\theta^{\pm})|^2/E^2})/2}$ ,  $v_{e/h} = \sqrt{(1 - \sqrt{1 - |\Delta(\theta^{\pm})|^2/E^2})/2}$ . We have also defined  $\theta^+ = \theta_S^e$ ,  $\theta^- = \pi - \theta_S^h$ , where the angles are defined in Fig. 2. In our study we have d-wave superconductors, thus  $\Delta(\theta^{\pm}) = \Delta \cos(2\theta^{\pm} - 2\gamma)$  and the macroscopic phase is  $e^{i\phi_{1/2}} = e^{i\phi_1/2} \frac{\Delta(\theta^{\pm})}{|\Delta(\theta^{\pm})|}$ . We choose the superconductor oriented along the 110 direction, implying  $\gamma = \pi/4$ .

In the normal region the eigenvector and corresponding momentum of a right moving electron with an incident angle  $\theta$  read:  $\psi_+^e = [1, e^{i\theta}, 0, 0]^T e^{ip^e \cos \theta x}$ ,  $p^e = (E + E_F)$ . A left moving electron is described by the substitution  $\theta \rightarrow \pi - \theta$ . If Andreev-reflection takes place, a left moving hole is generated with energy  $E$ , angle of reflection  $\theta_A$  and its corresponding wave function is given by  $\psi_-^h = [0, 0, 1, e^{-i\theta_A}]^T e^{-ip^h \cos \theta_A x}$ ,  $p^h = (E - E_F)$ . The transmission angles  $\theta$  and  $\theta_A$  for the electron-like and hole-like quasi-particles are given by  $q^e \sin \theta_S^e = p^e \sin \theta$  and  $q^e \sin \theta_S^e = p^h \sin \theta_A$ .

The full wave function in the type 1 scenario can be written as below for the various regions

$$\begin{aligned} \psi_{S_1} &= \Psi_{S_1+}^e + b_1 \Psi_{S_1-}^e + a_1 \Psi_{S_1-}^h, \quad x < 0, \\ \psi_N &= p \psi_+^e + q \psi_-^e + m \psi_+^h + n \psi_-^h, \quad 0 < x < d, \\ \psi_{S_2} &= c_1 \Psi_{S_2+}^e + d_1 \Psi_{S_2+}^h, \quad x > d. \end{aligned} \quad (3)$$

Matching the wave functions at the interfaces one can solve for the amplitudes of reflection  $a_1, b_1, c_1$  and  $d_1$ . Similarly, one can write the wave functions in case of type 2 scenario (hole incident from the right) and calculate the amplitudes  $a_2, b_2, c_2$ , and  $d_2$ . The detailed balance for the amplitudes are verified as follows

$$\begin{aligned} C a_1(\phi, E) &= C' a_2(-\phi, E), \\ b_i(\phi, E) &= b_i(-\phi, E) (i = 1, 2), \end{aligned} \quad (4)$$

with  $C = \frac{\Omega_{n-}}{|\Delta(\theta^-)|} \cos \theta_S^h$ , and  $C' = \frac{\Omega_{n+}}{|\Delta(\theta^+)|} \cos \theta_S^e$ . Following the procedure established in Ref.<sup>13</sup> and employing

analytic continuation  $E \rightarrow iw_n$  the dc Josephson current is calculated as

$$\begin{aligned}
I(\phi) &= \sum_{w_n} \frac{e}{2\beta\hbar} \int_{-\pi/2}^{\pi/2} \left[ \frac{a_1(\theta^+, \phi, iw_n)}{C'} \right. \\
&\quad \left. - \frac{a_2(\theta^+, \phi, iw_n)}{C} \right] \cos(\theta_S^e) d\theta_S^e, \\
&= \sum_{w_n} \frac{e}{2\beta\hbar} \int_{-\pi/2}^{\pi/2} \frac{|\Delta(\theta^+)|}{\Omega_{n,+}} [a_1(\theta^+, \phi, iw_n) \\
&\quad - a_1(\theta^+, -\phi, iw_n)] d\theta_S^e. \tag{5}
\end{aligned}$$

where  $\beta = 1/k_B T$ ,  $\Omega_{n,\pm} = \sqrt{w_n^2 + |\Delta(\theta^\pm)|^2}$  and  $w_n = \pi k_B T(2n+1)$ ,  $n = 0, \pm 1, \pm 2, \dots$

The above equation has a simple physical interpretation<sup>13</sup>. Andreev reflection is equivalent to the breaking up or creation of a Cooper pair. The scattering amplitude  $a_1$  describes the process in which an electron-like quasiparticle coming from the left superconducting graphene strip ( $x < 0$ ) is reflected as a hole-like quasiparticle. The amplitude  $a_2$  corresponds to the reverse process in which a hole-like quasiparticle is reflected as an electron-like quasiparticle. This implies that  $a_1$  and  $a_2$  correspond to the passage of a Cooper pair to the left and right respectively, hence, the dc Josephson current is proportional to  $a_1 - a_2$ . Further, the dc Josephson current is an odd function of the phase difference,  $\phi$ , as seen by the detailed balance condition,  $a_2(\phi, iw_n)/C = a_1(-\phi, iw_n)/C'$ . To calculate the Josephson current one thus takes the difference between the amplitudes  $a_1$  and  $a_2$  and then sums over the energies. In this approach we account for all the energies both bound states and the continuum. Eq.5 can be simplified as-

$$\begin{aligned}
I(\phi) &= \sum_{w_n} \frac{e}{2\beta\hbar} \int_{-\pi/2}^{\pi/2} \frac{|\Delta(\theta^+)|}{\Omega_{n,+}} [2iJ] d\theta_S^e, \text{ and} \\
J &= \frac{A \sin(\phi) + B \sin(2\phi)}{A' + 2B' \cos(\phi) + 2C' \cos(2\phi)} \tag{6}
\end{aligned}$$

In Eq.6,  $A, B, A', B'$ , and  $C'$  are functions of  $\theta^+, iw_n, E_f$  and  $d$ . The Free energy of the Josephson junction can then be calculated as

$$F(\phi) = \frac{1}{2\pi} \int_0^\phi I(\phi') d\phi'. \tag{7}$$

### III. $\pi$ -JUNCTION

Now we illustrate the results for the Josephson current as function of the length of the normal graphene interlude as well as the phase difference across the two superconducting graphene strips. The calculations are performed by treating Eqs. (5) and (7) numerically and the derived results hold for the  $T \rightarrow 0$  temperature limit. Fig. 3(a) shows the Josephson current as function of the Fermi energy, in the normal graphene strip, for different

lengths of the normal graphene layer. Note that Fermi energy is easily controllable in graphene. The plot shows that for extremely small length of normal graphene layer the Josephson current is negative for a wide range of Fermi energy, implying a  $\pi$  shift, while for larger intervening normal layers the Josephson current changes sign at larger values of the Fermi energy. One important fact to note is that for increased  $d$  the current decreases, which is in agreement with past Josephson works. Another observation from Fig. 3(a) is that at large Fermi energy the Josephson supercurrent becomes independent of  $E_f$ . The explanation for this is- when  $E_F \gg E, \Delta$ , the angles for electron and hole-like quasi-particles are  $\theta_S^e = \theta_S^h = \theta = -\theta_A$ . With this condition, the factor  $J$  from Eq.6, the Josephson supercurrent shorn of all prefactors, reduces to-

$$J = \frac{-ie^{-i\gamma} \sin(2\theta)}{E(\hbar^2 + e^{-2i\gamma} g^2)} \tag{8}$$

In the above equation,  $\gamma = (p_e + p_h)d \cos(\theta) = Ed \cos(\theta)$ ,  $h = (E - x)/2E$ ,  $g = (E + x)/2E$ ,  $x = \sqrt{E^2 - \sin^2(\theta)}$ . Thus in this limit the Josephson supercurrent becomes completely independent of  $E_F$ . Further, for  $d \rightarrow 0$  one can clearly see from Fig. 3(a) that the Josephson supercurrent becomes completely negative, this is also evident from Eq.8, wherein  $J$  reduces to  $-2w_n \sin(2\theta)/(2w_n^2 + \sin^2(2\theta))$ ,  $E = iw_n$ . Fig. 3(b) shows the current-phase relation for two different values of the Fermi energy. It again confirms the earlier indication of  $\pi$  shift. Finally, to establish beyond doubt that as function of Fermi energy one generates a  $\pi$  junction we plot the free energy in Fig. 3(c). The plot shows that as one changes the Fermi energy via a gate voltage one changes the ground state of the junction from 0 to  $\pi$ .

As shown in Fig. 3(c-d), the Free energy,  $F$ , has a minimum at  $\phi = \pi$  (for the  $\pi$  junction case) and the variation of  $F$  with  $\phi$  is strongly dependent on the length  $d$  and the Fermi energy. In this parameter regime the Free energy can be approximated as  $F \sim -E_\pi [\cos(\phi_\pi + \pi) + 1]$ , with  $E_\pi$  being the Josephson coupling constant. The 0 and  $\pi$  junctions, depicted in Fig. 1, have Josephson energies  $U_0 = E_0 |\sin(\phi_0/2)|$  and  $U_\pi = -E_\pi [\cos(\phi_\pi + \pi) + 1]$  plotted in Fig. 3(d). The superconducting phase difference is  $\phi_0$  for the 0 junction and  $\phi_\pi$  for the  $\pi$  junction. The total flux in the ring  $\Phi$  satisfies  $\phi_\pi - \phi_0 = 2\pi\Phi/\Phi_0 - 2\pi l$ , where  $\Phi_0$  is the flux quantum and  $l$  is an integer.

### IV. QUBITS AND GATES

In Ref. 14 the authors demonstrate a qubit with a  $\pi$  (SFS) junction<sup>15</sup> and a 0 (SNS) junction coupled into a ring. In our work we predict that our graphene based system, which does not need any ferromagnetic element in contrast to Ref.14, could implement a qubit. Further we show how to implement single qubit gates using our set up. The full Hamiltonian of the graphene ring system

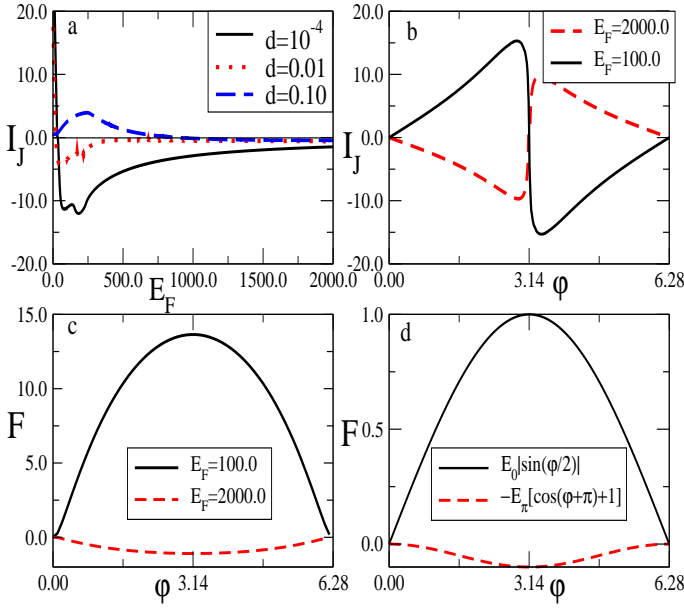


FIG. 3: (Color online) (a) Current (in units of  $e\Delta/\hbar$  and normalized by  $1/\beta$  throughout in all succeeding figures) versus Fermi energy,  $E_F$ , at phase difference  $\phi = \pi/2$ , for different values of width  $d$  (in units of  $\hbar v_F/\Delta$ ),  $U_0 = 100k_B T = 0.0001$  in this and all succeeding figures. (b) Current versus phase, where the length of normal graphene strip is  $d = 0.1$ , the dashed (RED) line is multiplied by a factor of ten for better visibility. (c) Free energy (normalized by  $1/\beta$ ) of  $G_S - G_N - G_S$  junction versus phase difference for different Fermi energies with 0 junction ( $E_F = 2000$  red dashed line) and  $\pi$  junction ( $E_F = 100$  black solid line) and length of normal graphene strip  $d = 0.1$ . (d) The approximate forms for the 0 and  $\pi$  junction energies are in good agreement with the real free energies and are used in analyzing the graphene Josephson qubit.

(Fig. 1) is given by  $H = K + U_{tot}$  with  $U_{tot} = U_0 + U_\pi + U_L$ , where  $U_L = (\Phi - \Phi_{ext})^2/2L_S$  is the magnetic energy stored in the ring and  $K$  is the flux independent kinetic energy. We next minimize the Hamiltonian with respect to flux and obtain  $\Phi(\phi_0) = \beta\Phi_0 \sin(\phi_\pi) + \Phi_{ext}$ , with  $\beta = 2\pi E_\pi L_S/\Phi_0^2$ . Substituting this equation in the expression for  $U_{tot}$ , we have:

$$\frac{U_{tot}}{E_\pi} = \alpha \left| \sin\left(\frac{\phi_\pi}{2} - \frac{\pi\Phi}{\Phi_0}\right) \right| + [\cos(\phi_\pi) - 1] + \pi\beta \sin^2(\phi_\pi). \quad (9)$$

with  $\alpha = E_0/E_\pi$ . For typical values mentioned in Fig. 4, we plot Eq. (9). We observe that the energy has double minima located approximately at  $\phi_\pi \sim 3\pi/5$  ( $|0\rangle$  state) and  $7\pi/5$  ( $|1\rangle$  state) which form the basis of the qubit. For single layer graphene with junction area<sup>16</sup>  $0.8 \times 10^{-12} \mu\text{m}^2$  and depth 1 nm, the electrostatic energy  $E_c$  is  $2.5 \times 10^{-24} \text{J}$ , while  $E_0$  the junction energy for the zero junction is around  $1000E_c$ . Thus for  $\alpha = 3.0$ , we have  $\Delta E$ , the energy gap, between the ground and first excited state  $\Delta E/h = 1000 \text{GHz}$ . The basic phase gate

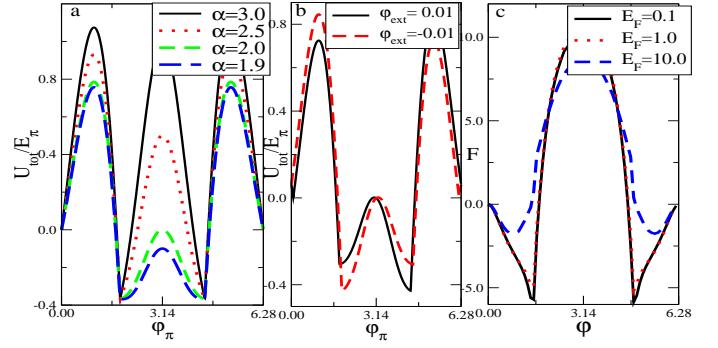


FIG. 4: (Color online) (a) Normalized energy,  $U_{tot}/E_\pi$ , as function of  $\phi_\pi$  for no external magnetic flux. (b) In presence of an external magnetic field with  $\alpha = 2.5$ . (c) The degenerate ground states of a d-wave Josephson junction.

with  $\phi = \Delta E \Delta t/\hbar = \pi$  could be implemented with gate time  $\Delta t$  given by 1 pico-second. In Fig. 4(c), the Free energy of a basic d-wave graphene Josephson junction is plotted for different values of Fermi energy and width  $d = 0.001$ . One can easily see that degenerate states are formed at  $\phi \sim \pi/2$  and  $3\pi/2$ . The coupling between these states can be easily varied by the gate voltage effectively realizing single qubit gates as aforementioned.

We will now show how to implement an exchange gate  $\sigma_x$  acting on the qubit states  $|0\rangle$  and  $|1\rangle$  for the structure as depicted in Fig. 1(a). This is realized by a tunnelling transition between the potential minima that encode these qubit states. Assuming the coupling potential is deep enough we approximate the qubit states by Gaussians centered at the minima of  $U_{tot}$ . By varying  $\alpha$  (or  $E_c$ ) one can induce tunnelling between the two minima in a controlled way. The exchange coupling of our system is calculated as

$$J = \int d\phi_\pi \Psi^*(\phi_\pi - \phi_{|0\rangle}) \left( -4E_c \frac{d^2}{d\phi_\pi^2} + U_{tot} \right) \Psi(\phi_\pi - \phi_{|1\rangle}). \quad (10)$$

In Fig. 5 we plot the exchange coupling versus the normalized Josephson energy for various values of the electrostatic energy,  $E_c$  in units of  $E_\pi$ . We see that for large  $\alpha$  no tunnelling occurs, while for  $\alpha \sim 3.0$  we obtain  $J \sim 10^{-6} E_\pi$  (for  $E_c = 0.01$ ) and, thus, the  $\sigma_x$  gate can be implemented in  $\Delta t \sim 10^{-6}$  seconds.

To conclude we have shown a novel implementation of a Josephson qubit using graphene as a substrate. Our work is the first to predict a qubit using only monolayer graphene. It was shown that a ferromagnetic graphene layer is unnecessary to create a  $\pi$ -shift, a completely novel result.  $\pi$  junctions have special role in a host of applications ranging from their use in superconducting digital circuits to superconducting qubits. We have shown how a  $\pi$  junction is formed in graphene where it can be very easily tuned by the application of a gate voltage alone. Secondly, we propose Josephson qubits and we present the phase and exchange gates for quantum computation purposes. Future proposals to make CNOT

or other two-qubit gate designs could also be envisaged using the above architecture.

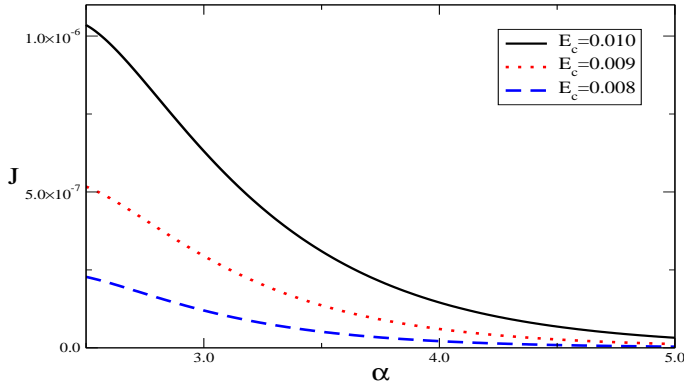


FIG. 5: (Color online) Exchange coupling  $J$  (in units of  $E_\pi$ ) as function of  $\alpha$  for different values of  $E_c$ . Here  $E_c \ll E_\pi$ .

## V. ACKNOWLEDGEMENTS

The authors acknowledge useful correspondence with Carlo Beenakker on a previous version of this manuscript. This work was supported by the EU grants EMALI and SCALA, EPSRC and the Royal Society.

- 
- <sup>1</sup> A. H. Castro Neto, F. Guinea, N. M. R. Peres, K. S. Novoselov and A. K. Geim, arXiv:0709.1163; A. K. Geim and K. S. Novoselov, *Nature Materials* **6**, 183 (2007).
  - <sup>2</sup> B. Trauzettel, D. V. Bulaev, D. Loss and G. Burkard, *Nature Physics* **3**, 192 (2007).
  - <sup>3</sup> A. A. Golubov, M. Yu. Kupriyanov and E. Il'ichev, *Rev. Mod. Phys.* **76**, 411 (2004).
  - <sup>4</sup> J. Q. You and F. Nori, *Physics Today*, p. 42, November (2005).
  - <sup>5</sup> A. Shailos, *Euro Phys. Lett.* **79**, 57008 (2007); P. Buset, A. Levy Yeyati and A. Martin-Rodero, *Phys. Rev. B* **77**, 205425 (2008).
  - <sup>6</sup> C. Benjamin, T. Jonckheere, A. Zazunov and T. Martin, *Eur. Phys. J. B* **57**, 279 (2007).
  - <sup>7</sup> J. Linder, T. Yokoyama, D. Huertas-Hernando and A. Sudbø, *Phys. Rev. Lett.* **100**, 187004 (2008).
  - <sup>8</sup> M. Titov, Ph. Jacquod and C. W. J. Beenakker, *Phys. Rev. B* **65**, 012504 (2002).
  - <sup>9</sup> M. Sgrist and T. M. Rice, *Rev. Mod. Phys.* **67**, 503 (1995); Y. Tanaka and S. Kashiwaya, *Phys. Rev. B* **53**, R11957 (1996).
  - <sup>10</sup> C. W. J. Beenakker, *Phys. Rev. Lett.* **97**, 067007 (2006).
  - <sup>11</sup> Y. Jiang, et. al. *Phys. Rev. B* **77**, 235420 (2008); S. Pathak, V. B. Shenoy and G. Baskaran, arXiv:0809.0244; A. M. Black-Schaffer and S. Doniach, *Phys. Rev. B* **75**, 134512 (2007).
  - <sup>12</sup> J. Linder and A. Sudbo, *Phys. Rev. Lett.* **99**, 147001 (2007); S. Bhattacharjee and K. Sengupta, *Phys. Rev. Lett.* **97**, 217001 (2006).
  - <sup>13</sup> A. Furusaki and M. Tsukada, *Solid State Comm.* **78**, 299 (1991); A. Furusaki, H. Takayanagi and M. Tsukada, *Phys. Rev. B* **45**, 10563 (1992).
  - <sup>14</sup> T. Yamashita, S. Tanikawa, S. Takahashi and S. Maekawa, *Phys. Rev. Lett.* **95**, 097001 (2005).
  - <sup>15</sup> A. I. Buzdin, *Rev. Mod. Phys.* **77**, 935 (2005); T. Noh, M. D. Kim and H.-S. Sim, arxiv:0804.0349.
  - <sup>16</sup> H. B. Heersche, et. al., *Nature* **446**, 56 (2007).